MOLECULAR IMAGING AND BIOLOGY

Mol Imaging Biol (2014) 16:255–263
DOI: 10.1007/s11307-013-0691-2

Published Online: 8 October 2013

World Molecular Imaging Society

RESEARCH ARTICLE

^{64}Cu- and ^{68}Ga-Labelled [Nle^{14}, Lys^{40}(Ahx-NODAGA)NH$_2$]-Exendin-4 for Pancreatic Beta Cell Imaging in Rats

Mikkola Kirsi,[1] Yim Cheng-Bin,[1] Fagerholm Veronica,[1] Ishizu Tamiko,[1] Elomaa Viki-Veikko,[1] Rajander Johan,[2] Jurttila Jori,[1] Saanijoki Tiina,[1] Tolvanen Tuula,[1] Tirri Marko,[1,3] Gourni Eleni,[4] Béhé Martin,[5] Gotthardt Martin,[6] Reubi Jean Claude,[7] Mäcke Helmut,[4] Roivainen Anne,[1,3] Solin Olof,[1,2] Nuutila Pirjo[1,8]

[1]*Turku PET Centre, University of Turku, Turku, Finland*
[2]*Accelerator Laboratory, Åbo Akademi University, Turku, Finland*
[3]*Turku Center for Disease Modeling, University of Turku, Turku, Finland*
[4]*Department of Nuclear Medicine, University Hospital Freiburg, Freiburg, Germany*
[5]*Center for Radiopharmaceutical Sciences ETH-PSI-USZ, Paul Scherrer Institute, 5232 Viiligen-PSI, Switzerland*
[6]*Department of Nuclear Medicine, Radboud University Nijmegen Medical Centre, Nijmegen, The Netherlands*
[7]*Division of Cell Biology and Exp. Cancer Research, Institute of Pathology, University of Berne, Berne, Switzerland*
[8]*Department of Endocrinology, Turku University Hospital, Turku, Finland*

Abstract

Purpose: Glucagon-like peptide-1 receptor (GLP-1R) is a molecular target for imaging of pancreatic beta cells. We compared the ability of [Nle^{14},Lys^{40}(Ahx-NODAGA-^{64}Cu)NH$_2$]-exendin-4 ([^{64}Cu]NODAGA-exendin-4) and [Nle^{14},Lys^{40}(Ahx-NODAGA-^{68}Ga)NH$_2$]-exendin-4 ([^{68}Ga]NODAGA-exendin-4) to detect native pancreatic islets in rodents.

Procedures: The stability, lipophilicity and affinity of the radiotracers to the GLP-1R were determined *in vitro*. The biodistribution of the tracers was assessed using autoradiography, *ex vivo* biodistribution and PET imaging. Estimates for human radiation dosimetry were calculated.

Results: We found GLP-1R-specific labelling of pancreatic islets. However, the pancreas could not be visualised in PET images. The highest uptake of the tracers was observed in the kidneys. Effective dose estimates for [^{64}Cu]NODAGA-exendin-4 and [^{68}Ga]NODAGA-exendin-4 were 0.144 and 0.012 mSv/MBq, respectively.

Conclusion: [^{64}Cu]NODAGA-exendin-4 might be more effective for labelling islets than [^{68}Ga]NODAGA-exendin-4. This is probably due to the lower specific radioactivity of [^{68}Ga]NODAGA-exendin-4 compared to [^{64}Cu]NODAGA-exendin-4. The radiation dose in the kidneys may limit the use of [^{64}Cu]NODAGA-exendin-4 as a clinical tracer.

Key words: Exendin, GLP-1R, Pancreas, Beta cell, PET, Rat

Introduction

Because of the high prevalence of diabetes in the human population, there is keen interest in developing imaging

Mikkola Kirsi and Yim Cheng-Bin contributed equally to this work.
Electronic supplementary material The online version of this article (doi:10.1007/s11307-013-0691-2) contains supplementary material, which is available to authorized users.

Correspondence to: Nuutila Pirjo; *e-mail:* pirjo.nuutila@utu.fi

agents that can be applied, *in vivo*, to study its pathophysiological mechanisms [1, 2]. Quantitative, noninvasive imaging of intact or transplanted pancreatic beta cells could provide a valuable tool for diagnosis and in monitoring the metabolic effects of therapeutic interventions.

Type 2 diabetes is accompanied by inefficiency of the glucagon-like peptide-1 receptor/glucagon-like peptide-1 (GLP-1R/GLP-1) system, which functions to reduce blood glucose levels by promoting insulin secretion and reducing glucagon secretion after a meal. In type 2 diabetes, both the secretion of GLP-1 and the affinity of GLP-1 to its receptor are impaired [3]. Exendin-4 is a subcutaneously administered GLP-1R agonist peptide that is used in the treatment of type 2 diabetes (exenatide; Byetta, Amylin/Lilly). It was the first of a class of incretin mimetics that showed potent glucoregulatory activity [4]. GLP-1R is found in pancreatic beta cells, with minimal or no expression in other islet cell types. Pancreatic ducts also express GLP-1R, but at lower levels as compared to beta cells [5, 6]. GLP-1R is overexpressed in virtually all benign insulinomas [7–9]. GLP-1R-targeted imaging with analogues of exendin labelled with radionuclides such as indium-111 (^{111}In) and technetium-99m (^{99m}Tc) for single-photon emission computed tomography (SPECT) [10, 11] and with gallium-68 (^{68}Ga), copper-64 (^{64}Cu) and fluorine-18 (^{18}F) for positron emission tomography (PET) [12–16] have been explored.

^{64}Cu ($t_{1/2}$=12.7 h, β^+_{max}=653 keV, β^+=17 %) and ^{68}Ga ($t_{1/2}$=68 min, β^+_{max}=1,899 keV, β^+>=89 %) are positron-emitting radiometals which can be used for the labelling of chelate-conjugated peptides. The long physical half-life of ^{64}Cu is optimal for preclinical investigations. The low energy of ^{64}Cu-derived positrons provides high spatial resolution for autoradiography and PET imaging. For human use, ^{68}Ga is generally preferred due to its availability, its low price and its short physical half-life which limits the radiation burden on the patient. The bifunctional chelator 1,4,7-triazacyclononane-1-glutaric acid-4,7-acetic acid (NODAGA) functions optimally for both ^{64}Cu and ^{68}Ga labelling [17].

In this study, we characterised and compared [^{64}Cu]NODAGA-exendin-4 and [^{68}Ga]NODAGA-exendin-4 for detecting native pancreatic beta cells. In the NODAGA-exendin-4 construct, Met^{14} was replaced by Nle. This modification allows labelling and short-time storage of the peptide without oxidation caused by air or by radiolysis. The stability, lipophilicity and affinity of the radiotracers were determined *in vitro*. Tracer tissue distribution, in rodents, was assessed by *ex vivo* autoradiography, by *ex vivo* biodistribution studies and by *in vivo* PET imaging. Finally, the estimated human radiation doses for the ^{64}Cu- and ^{68}Ga-labelled tracers were determined.

Materials and Methods

Peptides and Radiochemistry

The peptide sequence of NODAGA-exendin-4 (Electronic Supplementary Material (ESM) Online Resource 1) was HGEGTFTS DLSKQ&EEEAVRLFIEWLKNGGPSSGAPPPSK(#-NODAGA)NH_2, where &=norleucine, #=hexanoyl spacer (Peptide Specialty Laboratories). The peptide sequence of exendin-3 was DLSKQMEE EAVRLFIEWLKNGGPSSGAPPPS (Tocris Bioscience). The C-terminals of both peptides were amidated.

^{64}Cu in the form of [^{64}Cu]$CuCl_2$ was produced *via* the ^{64}Ni(p,n)^{64}Cu nuclear reaction, as previously described [18–20]. ^{64}Cu was formulated as 16 MBq/μl in 0.04 M HCl solution, and its effective specific radioactivity (ESA) was 2 TBq/μmol, as determined by titration with 1,4,8,11-tetraazacyclotetradecane-1,4,8,11-tetraacetic acid (Sigma-Aldrich). ^{68}Ga was obtained as [^{68}Ga]$GaCl_3$ from a ^{68}Ge/^{68}Ga generator (IGG100 1850 MBq, Eckert & Ziegler) by elution with 0.1 M HCl.

[^{64}Cu]NODAGA-exendin-4 was prepared by mixing [^{64}Cu]$CuCl_2$ (500 MBq, ESA 1,200±400 GBq/μmol) in 0.04 M HCl (40 μl) and NODAGA-exendin-4 (5 nmol in 5 μl deionised water) in 0.5 M ammonium acetate solution (pH 6). The reaction mixture (V_{total}= 500 μl) was incubated at 90 °C for 15 min. Quality control was performed using radio-HPLC (C_{12} column, Phenomenex). The HPLC conditions were: flow rate=1 ml/min, buffer A=0.1 % trifluoroacetic acid (TFA) in water, buffer B=0.1 % TFA in acetonitrile. Linear gradient was from 18 to 60 % buffer B in buffer A over 5 min.

[^{68}Ga]NODAGA-exendin-4 was prepared by mixing sodium acetate (18 mg, Merck) with 500 μl of [^{68}Ga]$GaCl_3$ (268±62 MBq, range=198–399 MBq) and the pH adjusted to approximately 3.5 with HCl. Subsequently, NODAGA-exendin-4 (5 nmol in 5 μl deionised water) was added and the reaction mixture was incubated at 95 °C for 15 min. The radiochemical purity was determined by radio-HPLC (C_{18} column, Phenomenex). The HPLC conditions were as described above, except that the linear gradient lasted 9 min.

[^{11}C]Methionine, which was used to verify the spatial location of the rat pancreas in PET imaging studies, was prepared using a previously reported method [21].

In Vitro Stability and Lipophilicity

[^{64}Cu]NODAGA-exendin-4 (30 MBq, 10 μl, 0.3 nmol) and [^{68}Ga]NODAGA-exendin-4 (30 MBq, 100 μl, 1.5 nmol) were incubated with 300 μl of human serum or phosphate-buffered saline (PBS, pH 7.4) at 37 °C. At selected time points, 50 μl aliquots were treated with acetonitrile (50 μl) to precipitate the serum proteins. After centrifugation (8 min, 10,000×*g*), the supernatant was analysed using radio-HPLC (C_{12} column, Phenomex) with a 5-min linear gradient.

The octanol/water partition coefficients of the ^{64}Cu- and ^{68}Ga-labelled peptides (N=17 and N=7, respectively) were measured by vortex mixing 500 μl of 1-octanol and 500 μl PBS (pH 7.4) with approximately 0.1 MBq of radiolabelled peptide for 2–3 min. Following centrifugation at 16,000×*g* for 8 min, samples from the organic and aqueous phases were analysed using a γ-counter (1480 Wizard 3″ Gamma Counter, PerkinElmer). Log(D)$_{octanol/water}$ was calculated as log([radioactivity]$_{octanol}$/[radioactivity]$_{water}$).

Synthesis of [Nle^{14},Lys^{40}(Ahx-NODAGA-^{nat}Cu)NH_2]-Exendin-4 and [Nle^{14},Lys^{40}(Ahx-NODAGA-^{nat}Ga)NH_2]-Exendin-4

A mixture of NODAGA-exendin-4 (crude peptide, 10.1 mg, ~0.002 mmol) in ammonium acetate buffer (pH 5.4, 0.5 M, 500 μl) and

an aliquot (6.7 µl, ~0.002 mmol) of an aqueous solution of $^{nat}CuCl_2 \times 2H_2O$ 0.3 M was allowed to react at room temperature for 3.5 h. By then, the complex formation checked by analytical HPLC (EC 250/4.6 Nucleosil 120-5 C18 column; eluents: A=0.1 % TFA in H_2O and B= acetonitrile; gradient: 15 % B to 90 % B in 28 min; flow rate, 1 ml/min) was complete. The elution time difference between the product and the starting material was 40 s using the same gradient. [Nle^{14},Lys^{40}(Ahx-NODAGA-^{nat}Cu)NH_2]-exendin-4 ([^{nat}Cu]NODAGA-exendin-4) was purified by preparative HPLC and 3.3 mg of the pure complex was isolated. Quality control of the ^{nat}Cu-containing complex was carried out by analytical HPLC following the conditions described above where only one single peak was detected. The observed monoisotopic peak $[M+H]^+$ 4,826.9 for the ^{nat}Cu-containing complex corresponds with the calculated value of 4,825.9.

A mixture of NODAGA-exendin-4 (crude peptide, 13.5 mg, ~0.0028 mmol) in sodium acetate buffer (pH 4.0, 0.2 M, 1 ml) and an aliquot (24 µl, ~0.0071 mmol) of an aqueous solution of $^{nat}Ga(NO_3)_3 \times H_2O$ 0.3 M was heated at 95 °C for 10 min. By then, the complex formation was checked by analytical HPLC as previously described. The difference in the elution time between the product and the starting material was 30 s under the same conditions. The free metal ions, as well as the impurities from the final product, were initially removed by SepPak C-18 purification (Waters), followed by preparative HPLC, and 2.4 mg of the pure [Nle^{14},Lys^{40}(Ahx-NODAGA-^{nat}Ga)NH_2]-exendin-4 ([^{nat}Ga]NODAGA-exendin-4) complex was isolated. The observed monoisotopic $[M+H]^+$ 4,833.6 for the ^{nat}Ga-containing complex corresponds with the calculated value of 4,832.1. The analytical HPLC quality control of the pure complex showed only one single peak.

Characterization of GLP-1 Receptor Binding Affinity for [^{nat}Cu]- and [^{nat}Ga]NODAGA-Exendin-4

The binding affinities of the two exendin analogues and GLP-1 as a control were evaluated in competition-binding experiments performed *in vitro* in GLP-1R-expressing human insulinomas using autoradiography, as reported previously [7, 8]. For each of the tested compounds, complete competition binding experiments with [^{125}I]GLP-1(7-36) amide (74 GBq/µmol; Anawa) and increasing concentrations of the unlabelled peptides ranging from 0.1 to 1,000 nM were performed in triplicate. IC_{50} values were calculated of the data using a computer-assisted image processing system as described previously [8].

Experimental Animals

Male Sprague–Dawley rats (N=41) weighing 292±29 g were obtained from the Central Animal Laboratory, University of Turku. The experimental protocol was approved by the National Animal Experiment Board.

Ex Vivo Biodistribution

Rats were anaesthetised with isoflurane and intravenously injected with 96±38 MBq/kg [^{64}Cu]NODAGA-exendin-4 at a specific radioactivity of 81±43 GBq/µmol and mass 1.9±1.7 nmol/kg (range=0.3–5.9 nmol/kg, 9.1±8.3 µg/kg) or with 112±23 MBq/kg [^{68}Ga]NODAGA-exendin-4 at a specific radioactivity of 12.7±1.6 GBq/µmol and mass 9.1±3.0 nmol/kg (range=5.4–14.6 nmol/kg, 43.7±14.7 µg/kg). At various time points post-injection (p.i.), the animals were deeply anaesthetised with isoflurane. Blood was collected by cardiac puncture and the tissues of interest (Table 1) weighed and measured for radioactivity using a γ-counter. The GLP-1R specificity of the radiopeptides in rats was assessed at 1 h p.i. in separate groups of animals by intravenous injection of an excess of unlabelled exendin-3, administered immediately before the radiopeptide injection.

Radioactivity measurements were corrected for radionuclide decay. The radioactivity remaining in the tail was subtracted from the amount of radioactivity injected. Finally, tissue uptake of radioactivity was reported as a percentage of the injected dose of radioactivity per gram of tissue (%ID/g).

Autoradiography

A piece of the pancreas was frozen in isopentane. Frozen sections (20 µm) were dried under a fan and apposed to imaging plates (Fuji BAS-TR2025, Fuji Photo Film Co.) for approximately two isotope half-lives. In addition, the gastrointestinal channel was emptied and the stomach and the caecum were unfolded. The gastrointestinal channel was covered with cling film and apposed to an imaging plate for autoradiography as described above.

The digital images were analysed using the AIDA 4 software (Raytest). Three pancreatic sections per rat were analysed. The mean density values (photostimulated luminescence per square millimetres) of ten prominently labelled islets and of the exocrine tissue were determined and corrected for background. Finally, the islet-to-exocrine tissue ratio was calculated. Islet localisation was verified by insulin immunohistochemistry. The radioactivity in the gastrointestinal region was analysed similarly by outlining regions of interest and calculating regional signal ratios.

Metabolite Analysis

Radioactive metabolites in serum, urine, pancreas and kidney were assessed using radio-HPLC (C_{12} column, Phenomex) as described above. Samples were collected at 5 min, 1 h, 18 h and 40 h after [^{64}Cu]NODAGA-exendin-4 injection and at 1 h after [^{68}Ga]NODAGA-exendin-4 injection. Serum and urine were treated with acetonitrile (1:1, *v*/*v*), centrifuged 2×5 min at 12,000×*g* and the supernatant analysed. Representative pancreas and kidney samples (0.14±0.05 g) were homogenised in 500 µl PBS (pH 7.4), centrifuged for 5 min at 12,000×*g*, treated with acetonitrile (1:1, *v*/*v*) and centrifuged for 2×5 min at 12,000×*g*. The supernatant was used for analysis.

PET Imaging

Whole-body distribution kinetics of intravenously administered exendin-4 was evaluated using an Inveon Multimodality PET/CT (Siemens Medical Solutions). Following the CT scan for attenuation correction, a PET scan was acquired in 3D list mode with an energy window of 350–650 keV. Separate groups of animals were injected with 81±17 MBq/kg [^{64}Cu]NODAGA-exendin-4 (N=5; specific radioactivity, 74±38 GBq/µmol; mass, 1.4±0.8 nmol/kg),

Table 1. Biodistribution of [^{64}Cu]NODAGA-exendin-4 in rats (in percentage of the injected dose of radioactivity per gram of tissue)

Organ	5 min (N=3)	1 h (N=9)	18 h (N=3)	40 h (N=3)	1 h blocking Ex-3 1 mg/kg[a] (N=5)	1 h blocking Ex-3 7 mg/kg[a] (N=3)
Adipose tissue	0.09±0.02***	0.02±0.01	0.02±0.01	0.005±0.003	0.03±0.01	0.015±0.004
Blood	0.74±0.08***	0.08±0.02	0.03±0.01	0.03±0.01	0.13±0.07	0.10±0.04
Blood cells	0.12±0.01	0.015±0.003	0.38±0.65	0.012±0.004	0.02±0.01	0.02±0.01
Brain	0.023±0.002***	0.004±0.001	0.01±0.01	0.004±0.002	0.006±0.003	0.004±0.001
Heart	0.30±0.04***	0.04±0.01	0.03±0.01	0.04±0.01	0.06±0.03	0.04±0.01
Kidney	13±2***	30±4	17±7**	9±7***	21±10	25±2
Liver	0.30±0.09**	0.14±0.04	0.15±0.04	0.12±0.05	0.17±0.08	0.16±0.10
Lung	3.9±2.1	3.5±1.2	2.33±0.96	1.0±0.5*	0.24±0.06▲▲▲	0.16±0.05▲▲▲
Muscle	0.15±0.06***	0.02±0.01	0.011±0.002	0.01±0.01	0.03±0.01	0.016±0.002
Pancreas	0.31±0.01***	0.09±0.02	0.04±0.04*	0.04±0.02*	0.07±0.04	0.04±0.01
Serum	1.30±0.13***	0.15±0.03	0.04±0.03*	0.04±0.01*	0.24±0.14	0.20±0.08
Spleen	0.18±0.03***	0.06±0.01	0.05±0.01	0.04±0.02	0.06±0.02	0.07±0.04
Stomach wall	1.08±0.60	0.88±0.40	0.34±0.43	0.28±0.24	0.15±0.05▲▲	0.10±0.01▲▲

One-way ANOVA and Bonferroni's multiple comparison test
▲/*P<0.05; ▲▲/**P<0.01; ▲▲▲/***P<0.001 (statistically significant compared to [^{64}Cu]NODAGA-exendin-4 at 1 h post-injection)
[a]Co-injection of an excess of unlabelled exendin-3

or with 136±60 MBq/kg [^{68}Ga]NODAGA-exendin-4 (N=3; specific radioactivity, 13±3 GBq/μmol; mass, 10.4±2.6 nmol/kg) or with [^{11}C]methionine 34±48 MBq/kg. Dynamic imaging lasts for 60 min starting from the time of injection of [^{64}Cu]NODAGA-exendin-4 and [^{68}Ga]NODAGA-exendin-4. Visualisation of the pancreas using [^{11}C]methionine PET was performed in three of the five animals imaged with [^{64}Cu]NODAGA-exendin-4 using two different study protocols. Dynamic [^{11}C]methionine data were collected either for 30 min immediately prior to a [^{64}Cu]NODAGA-exendin-4 120-min PET scan (N=1) or dynamic 40-min [^{11}C]methionine data were collected the day before a [^{64}Cu]NODAGA-exendin-4 60-min PET scan (N=2).

The PET data were reconstructed using the ordered-subset expectation maximization OSEM 2D algorithm. Quantitative analyses were performed using Inveon Research Workplace 3 software (Siemens Medical Solutions) by defining the volumes of interest (VOIs) on selected tissues. Skeletal muscle was used as a reference tissue. The VOIs for the pancreas were defined in the [^{11}C]methionine images and copied onto the corresponding [^{64}Cu]NODAGA-exendin-4 images. Time–activity curves (TACs) were extracted from the dynamic images. The radioactivity retained in the tail was subtracted from the injected dose. The radioactivity uptake, corrected for radionuclide decay to the time of injection, was expressed as a standardised uptake value (SUV). SUV_{bw} was calculated as the ratio of tissue radioactivity concentration at time (t), $c(t)$ and the injected radioactivity dose at the time of injection divided by body weight: $SUV_{bw}=c(t)/(\text{injected dose/body weight})$.

Estimation of Radiation Doses for Humans

Absorbed doses were calculated with the OLINDA/EXM 1.0 software [22, 23] which includes radionuclide information and a selection of human body phantoms. Rat *ex vivo* biodistribution results and PET imaging results were integrated as area under the time–activity curves. The obtained residence times were converted into corresponding human values by multiplication with organ-specific factors to scale organ and body weights: $(W_{TB,rat}/W_{Organ,rat})\times(W_{Organ,human}/W_{TB,human})$, where $W_{TB,rat}$ and $W_{TB,human}$ are the body weights of rat and human (70-kg male), respectively, and $W_{Organ,rat}$ and $W_{Organ,human}$ are the organ weights of rat and human (70-kg male), respectively.

Statistical Analysis

Statistical analyses were performed using GraphPad Prism 4 and 5 (GraphPad Software). Results are reported as the mean±SD. Two-tailed, unpaired Student's t test and one-way or two-way ANOVA were used for the analyses of statistical differences between groups. Values of P<0.05 were considered statistically significant.

Results

Radiochemistry

The specific radioactivity for [^{64}Cu]NODAGA-exendin-4 was 90±10 GBq/μmol at the end of synthesis, with a radiochemical purity of 93±4 %. The corresponding values for [^{68}Ga]NODAGA-exendin-4 were 20±5 GBq/μmol and 98.0±0.3 %.

In Vitro Tests

After 3 h incubation in PBS and serum, the stability of both [^{64}Cu]- and [^{68}Ga]NODAGA-exendin-4 exceeded 91 %. At 24 h, the radioactivity associated with [^{64}Cu]NODAGA-exendin-4 still exceeded 82 %. These results indicate that peptides were highly stable *in vitro*. The Log(D) values for [^{64}Cu]- and [^{68}Ga]NODAGA-exendin-4 were −0.92±0.37 and −2.38±0.37, respectively. These results indicate that both compounds have low lipophilicity. The IC_{50} values were 1.0±0.2 nM for GLP-1, 2.70±0.62 nM for [^{nat}Cu]NODAGA-exendin-4 and 2.17±0.42 nM for [^{nat}Ga]NODAGA-exendin-4.

Ex Vivo Whole-Body Biodistribution

The biodistribution of ^{64}Cu and ^{68}Ga radioactivity at different time points after tracer injection in rats is presented in Fig. 1 and in Table 1. The radioactivity was rapidly cleared from the blood circulation. At all investigated time points, the highest levels of ^{64}Cu and ^{68}Ga radioactivity were observed in the kidneys, peaking at approximately 30 %ID/g at 1 h after tracer injection (Table 1). At 40 h, the kidneys still retained almost 10 %ID/g of the [^{64}Cu]NODAGA-exendin-4 radioactivity. After 1 hour, uptake was also rather high in the lung (3.5±1.1 %ID/g for [^{64}Cu]NODAGA-exendin-4 and 0.7±0.2 for [^{68}Ga]NODAGA-exendin-4) and stomach wall (0.9±0.4 %ID/g and 0.23±0.06, respectively). Pancreatic uptake at 1 h was 0.04±0.01 %ID/g for [^{68}Ga]NODAGA-exendin-4 and 0.09±0.02 %ID/g for [^{64}Cu]NODAGA-exendin-4 and was reduced to 0.04±0.02 %ID/g at 40 h after injection. In the lung, pancreas and stomach wall, the uptake of [^{68}Ga]NODAGA-exendin-4 was significantly lower than the corresponding uptake of [^{64}Cu]NODAGA-exendin-4 (Fig. 1). An excess of unlabelled exendin-3 significantly reduced the uptake of [^{64}Cu]NODAGA-exendin-4 in the lung and stomach wall (Table 1), suggesting that tracer uptake was GLP-1R-specific in these tissues. Similar results were observed for [^{68}Ga]NODAGA-exendin-4 (N=1; results not shown).

Biodistribution in the Pancreas and Gastrointestinal Region

[^{64}Cu]NODAGA-exendin-4 and [^{68}Ga]NODAGA-exendin-4 labelled GLP-1R in pancreatic islets at all investigated time points (Figs. 2 and 3). The islet-to-exocrine tissue ratio in rat pancreas at 60 min p.i. was higher for [^{64}Cu]NODAGA-exendin-4 than for [^{68}Ga]NODAGA-exendin-4 (Fig. 3b). Islet labelling was GLP-1R-specific, as indicated by a reduced islet-to-exocrine [^{64}Cu]NODAGA-exendin-4 signal after co-injection of exendin-3 (1 mg/kg, P<0.05, and 7 mg/kg, P<0.001, Kruskal–Wallis one-way ANOVA with Dunn's *post hoc* test). Pancreatic uptake of ^{64}Cu radioactivity at the whole-tissue level, determined by *ex vivo* measurements, was 0.09±0.02 %ID/g at 60 min p.i. The islet-to-exocrine ratio of [^{64}Cu]NODAGA-exendin-4 radioactivity was 106±63.

GLP-1R-specific labelling was detected as a narrow band in the proximal duodenum (Fig. 4) and in the glandular stomach. [^{64}Cu]- and [^{68}Ga]NODAGA-exendin-4 labelling in the remainder of the gastrointestinal region was weak and homogenous.

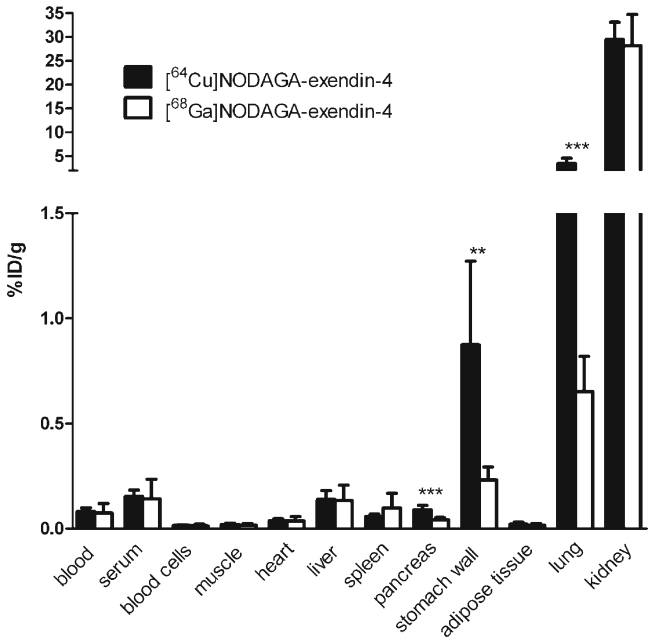

Fig. 1. Tissue distribution of [^{64}Cu]NODAGA-exendin-4 (N=9) and [^{68}Ga]NODAGA-exendin-4 radioactivity (N=6) 1 h post-injection. **P<0.01; ***P<0.001 (Student's t test).

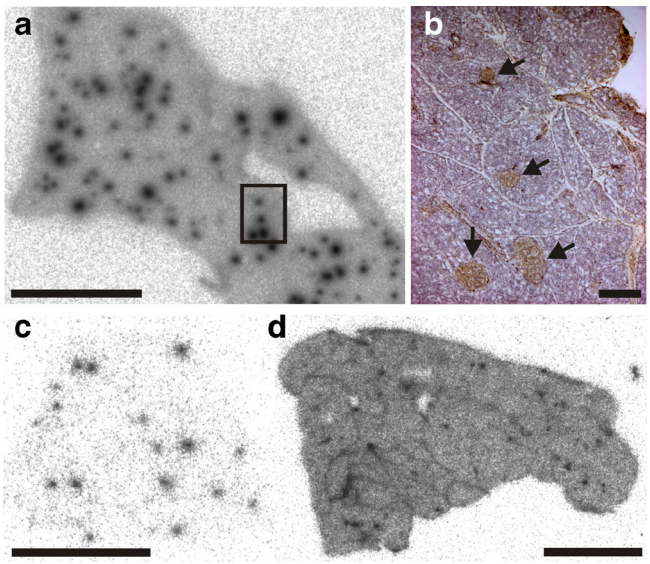

Fig. 2. Labelling of islets in rat pancreatic tissue sections at 1 h after the injection of [^{64}Cu]NODAGA-exendin-4 or [^{68}Ga]NODAGA-exendin-4. **a** [^{64}Cu]NODAGA-exendin-4. **b** Close-up of the boxed region in (**a**) after staining of the islets (*arrows*) with insulin. **c** [^{68}Ga]NODAGA-exendin-4. **d** Co-injection of a high dose of exendin-3 (7 mg/kg) with [^{64}Cu]NODAGA-exendin-4 reduced islet labelling, indicating that the labelling was GLP-1R-specific. *Scale bars* in (**a**), (**c**) and (**d**) are 5 mm; *scale bar* in (**b**) is 0.5 mm.

In Vivo Stability

There were no major differences between the *in vivo* metabolism of [^{64}Cu]NODAGA-exendin-4 and [^{68}Ga]NODAGA-exendin-4 (ESM Online Resource 2 and 3). At 1 h p.i., 55±12 % of the ^{64}Cu and 70±5 % of the ^{68}Ga radioactivity corresponded to the unchanged tracer in serum. In the kidney and urine, only minimal amounts of intact tracer were detected, whereas in pancreas, 44±13 % of the ^{64}Cu radioactivity and 32±5 % of the ^{68}Ga radioactivity represented intact tracer.

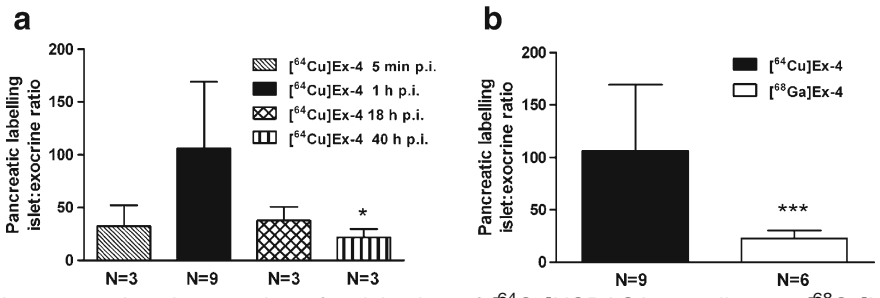

Fig. 3. Pancreatic islet-to-exocrine tissue ratios after injection of [^{64}Cu]NODAGA-exendin-4 or [^{68}Ga]NODAGA-exendin-4. **a** Labelling of islets after injection of [^{64}Cu]NODAGA-exendin-4. **b** Washout of the signal was observed at 40 h post-injection (Kruskal–Wallis one-way ANOVA with Dunn's *post hoc* test: $P<0.05$). Islet labelling at 1 h post-injection was higher for [^{64}Cu]NODAGA-exendin-4 than for [^{68}Ga]NODAGA-exendin-4 (Mann–Whitney *U* test: $P<0.001$). *$P<0.05$; **$P<0.01$; ***$P<0.001$.

PET Imaging

TACs after injection of [^{64}Cu]NODAGA-exendin-4 and [^{68}Ga]NODAGA-exendin-4 are shown in Figs. 5 and 6. The radioactivity of the kidneys exceeded the radioactivity of all other organs already at 5 min p.i. One hour after injection, the SUVs of [^{64}Cu]NODAGA-exendin-4 and [^{68}Ga]NODAGA-exendin-4 in the kidneys were 41±4 and 30±3, respectively. With neither tracer was the pancreas visualised in the PET images. Using [^{11}C]methionine PET images as an anatomical reference for the pancreas localisation, the pancreatic SUV of [^{64}Cu]NODAGA-exendin-4 was 0.63±0.04. Pancreas-to-muscle and kidney-to-pancreas ratios were 3.4±0.2 and 65±4, respectively. The corresponding ratios according to *ex vivo* measurements were 5±1 and 350±110. The apparently higher pancreatic tracer uptake determined by PET, as compared to the *ex vivo* measurements, was associated with a spillover signal from the kidneys in PET images. The [^{64}Cu]NODAGA-exendin-4 SUV in the stomach wall was 4.1±0.3 and in the lung was 1.8±0.7. The [^{68}Ga]NODAGA-exendin-4 SUV in the lung was 0.46±0.04. The stomach wall could not be identified in [^{68}Ga]NODAGA-exendin-4 PET images.

Dosimetry

Extrapolated from the rat *ex vivo* results, the mean [^{64}Cu]NODAGA-exendin-4 effective dose for a 70-kg human adult was 0.074 mSv/MBq (ESM Online Resource 4). Estimated from the PET imaging results, the mean effective doses were 0.144 mSv/MBq for [^{64}Cu]NODAGA-exendin-4 and 0.012 mSv/MBq for [^{68}Ga]NODAGA-exendin-4. The kidney was the dose-limiting organ. Calculated from the *ex vivo* results, the absorbed kidney dose for [^{64}Cu]NODAGA-exendin-4 was 1.48 mSv/MBq. Based on the PET results, the corresponding value for [^{64}Cu]NODAGA-exendin-4 was 3.95 mSv/MBq and for [^{68}Ga]NODAGA-exendin-4 was 0.523 mSv/MBq.

Discussion

Exendin-4-based radiotracers are considered promising tools for *in vivo* imaging of the GLP-1R using SPECT and PET. Possible clinical applications include the localisation of insulinomas and transplanted beta cells, as demonstrated in humans with [^{111}In]DOTA(tetraazacyclododecantetraacetic acid)-exendin-4

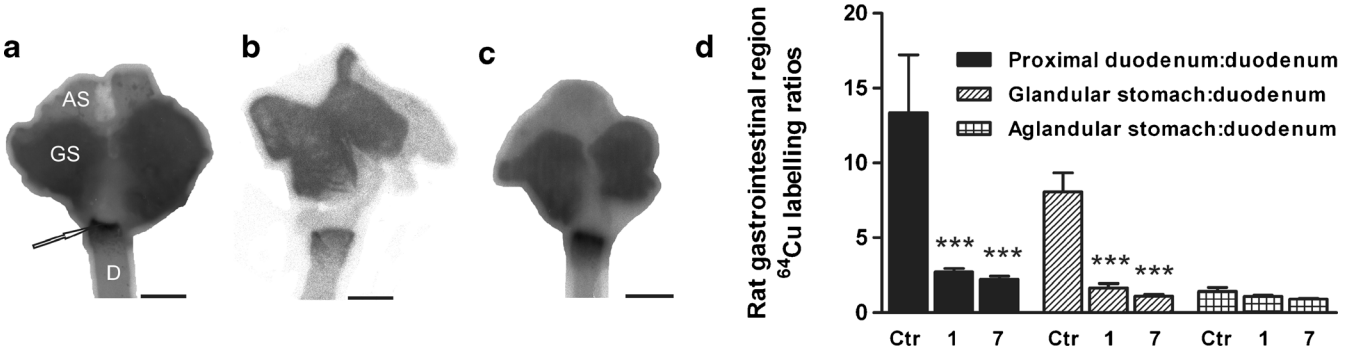

Fig. 4. Autoradiography images and analysis of rat gastrointestinal region. Rat gastrointestinal region at 1 h (**a**), at 40 h (**b**) post-injection of [^{64}Cu]NODAGA-exendin-4 and 1 h after injection of [^{68}Ga]NODAGA-exendin-4 (**c**). In the proximal duodenum, a band of high radioactivity was observed (indicated by an *arrow*). **d** Autoradiography analysis of [^{64}Cu]NODAGA-exendin-4 labelling in rat at 1 h post-injection of the tracer alone (*Ctr*, $N=4$) or after co-injection of exendin-3 (1 mg/kg, $N=4$, or 7 mg/kg, $N=3$). Exendin-3 reduced the labelling in the proximal duodenum and in the glandular stomach (two-way ANOVA with Bonferroni's *post hoc* tests: ***$P<0.001$), indicating that labelling in these regions was GLP-1R-specific. *AS* aglandular stomach, *D* duodenum, *GS* glandular stomach. *Scale bars*, 10 mm.

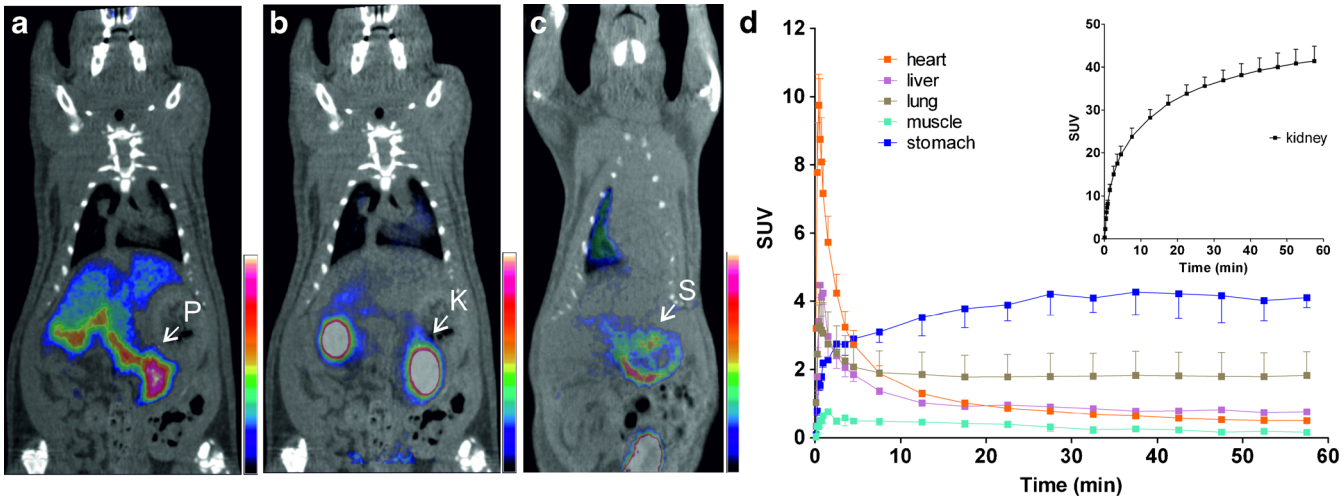

Fig. 5. Representative coronal PET/CT images of a rat, first imaged with [^{11}C]methionine (**a**) to identify the pancreas (sum image 0–30 min post-injection) and thereafter with [^{64}Cu]NODAGA-exendin-4 (sum image 2–2.5 h post-injection) (**b**). [^{64}Cu]NODAGA-exendin-4 uptake in the stomach wall was easily distinguishable in the PET images (**c**), but pancreas was not detectable (sum image 40–60 min post-injection). TACs were determined by defining VOIs on selected tissues (**d**). The kidney (*K*), pancreas (*P*) and stomach (*S*) are indicated by *arrows*.

and [^{111}In]DTPA(diethylenetriaminepentacetic acid)-exendin-4 SPECT [9, 24–26]. In the present study, we compared the labelling of native pancreatic islets by [^{64}Cu]NODAGA-exendin-4 and [^{68}Ga]NODAGA-exendin-4 in rats.

We found GLP-1R-specific exendin-4 labelling in the lung, stomach wall, proximal duodenum and pancreatic islets. Interestingly, the reduction in tracer uptake induced by an excess of unlabelled exendin-3 could only be detected using autoradiography. At the whole-organ level measured by γ-counting, exendin-3 had no significant effect on the pancreatic uptake of the radiotracer. This is explained by the fact that beta cells constitute only 1–2 % of the pancreatic volume. The feasibility of quantitative *in vivo* imaging of native pancreatic beta cells is still an issue of debate [27, 28]. Theoretical estimates suggest

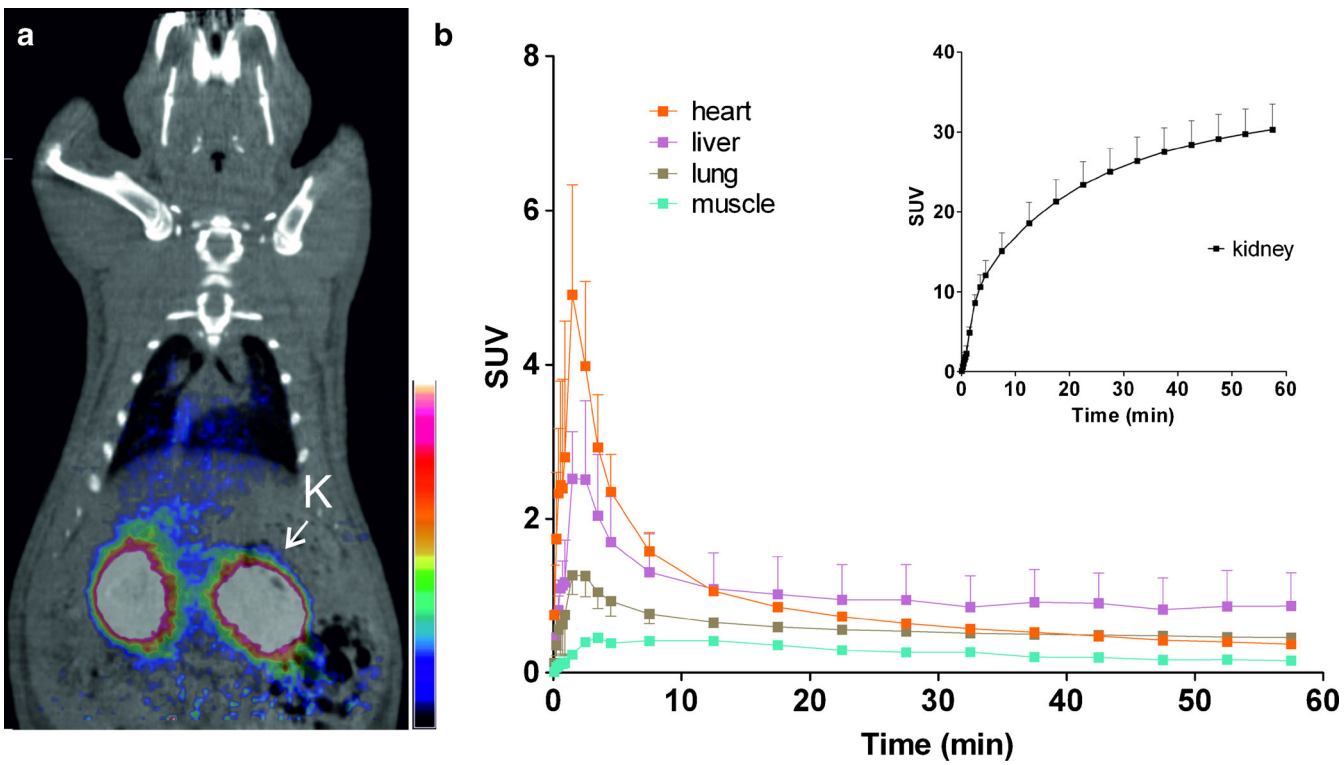

Fig. 6. **a** Representative coronal PET/CT image of a rat imaged with [^{68}Ga]NODAGA-exendin-4 (sum image 45–60 min post-injection). **b** The pancreas was not detectable after injection of [^{68}Ga]NODAGA-exendin-4. TACs were determined by drawing VOIs on selected tissues. The kidney (*K*) is indicated by an *arrow*.

that a successful imaging agent for native beta cells would require an islet-to-exocrine tissue signal ratio of approximately 1,000:1 [29]. The islet-to-exocrine tissue ratios determined in rats using autoradiography were 106±63 for [^{64}Cu]NODAGA-exendin-4 and 23±3 for [^{68}Ga]NODAGA-exendin-4. It is thus conceivable that these islet-to-exocrine ratios were too low to allow the detection of GLP-1R at the whole-tissue level in biodistribution studies and in PET images. In a very recent publication, using gallium-68-labelled exendin-4 in a similar manner to us, Selvaraju *et al.* [30] failed to visualise the pancreas using PET imaging in rodents. However, they were able to demonstrate specific uptake in the pancreas using *ex vivo* gamma counting.

Autoradiography of the rat gut revealed GLP-1R-specific [^{64}Cu]- and [^{68}Ga]NODAGA-exendin-4 labelling in the glandular stomach and in a distinct narrow band in the proximal-most duodenum. The labelling of the stomach wall probably represents GLP-1R on parietal cells [31]. GLP-1 has been reported to stimulate H^+ production in isolated rat parietal cells *in vitro* [32]. The direct stimulatory effect of GLP-1 on parietal cells is opposite to the inhibitory effect on gastric acid secretion in response to systemic GLP-1 that occurs *via* an indirect vagally mediated mechanism [33]. The physiological function of the GLP-1R cluster in the proximal duodenum is unknown. It can be speculated that the high uptake of [^{111}In]DOTA-exendin-4 in the human proximal duodenum observed by Christ and co-workers [25] in two out of six insulinoma patients scanned with SPECT corresponds to the proximal duodenal GLP-1R cluster found in the present study in rats. In rat lung, high levels of GLP-1R have consistently been reported, whereas in human lung, GLP-1R levels are very low [8].

After intravenous injection, exendin radiotracers are rapidly cleared from the blood. This promotes a favourable target-to-background signal ratio. However, most of the radioactivity accumulates in the kidney cortex *via* peptide uptake mechanisms independent of the GLP-1R [34]. The spillover signal from the highly radioactive kidneys hampers the evaluation by PET of the radioactivity levels in the adjacent significantly less radioactive pancreas, especially in small animals. This is unfortunate from the pancreatic imaging point of view. Accordingly, we were not able to visualise the pancreas in the PET images. Moreover, the kidney is an organ that is sensitive to radiation [35]. In clinical studies, there is a risk that the radiation burden on the kidneys may become unacceptably high. In the kidneys, the uptakes of [^{64}Cu]NODAGA-exendin-4 and [^{68}Cu]NODAGA-exendin-4 were similar. However, because of the longer physical half-life of copper-64 (12.7 h) compared to gallium-68 (68 min), the radiation burden of [^{64}Cu]NODAGA-exendin-4 significantly exceeded that of [^{68}Ga]NODAGA-exendin-4.

All GLP-1R-positive organs investigated accumulated significantly more [^{64}Cu]NODAGA-exendin-4 than [^{68}Ga]NODAGA-exendin-4 radioactivity. This difference cannot be explained by stability issues since [^{68}Ga]NODAGA-exendin-4 actually appeared somewhat more stable than [^{64}Cu]NODAGA-exendin-4 *in vivo*. Receptor affinities of both metallopeptides are in the low nanomolar range; the replacement of Met^{14} by Nle^{14} appears not to have an influence on GLP-1R binding affinity. The higher specific radioactivity and subsequent lower injected mass of [^{64}Cu]NODAGA-exendin-4 compared to [^{68}Ga]NODAGA-exendin-4 may account for the higher GLP-1R-specific uptake of the former. The lower positron energy of ^{64}Cu is likely to contribute to the better quality of [^{64}Cu]NODAGA-exendin-4 autoradiographs of pancreatic islets as compared to [^{68}Ga]NODAGA-exendin-4 autoradiographs.

Conclusions

In summary, both copper-64- and gallium-68-labelled NODAGA-exendin-4 tracers specifically labelled rat pancreatic islets. Autoradiography results suggest that [^{64}Cu]NODAGA-exendin-4 might be more effective for beta cell imaging than [^{68}Ga]NODAGA-exendin-4. However, these tracers could not be used to detect beta cells in rodent pancreas with PET. The long physical half-life (12.7 h) of copper-64 enables long study protocols and makes it practical for preclinical investigations. However, the high radiation burden on the kidneys may limit its use as a clinical tracer.

Acknowledgments. The authors thank Dr. Jörn Schlesinger for technical expertise and scientific discussions and Vesa Oikonen MSc for helping with PET/CT data analysis. Aake Honkaniemi, Elisa Riuttala, Merja Tuomas and Marko Vehmanen are acknowledged for their technical assistance. The study was conducted within the Finnish Centre of Excellence in Molecular Imaging in Cardiovascular and Metabolic Research, financially supported by the Academy of Finland, the University of Turku, Turku University Hospital and Åbo Akademi University. The research leading to these results has received funding from the European Community's Seventh Framework Programme (FP7/2007-2013) under grant agreement 222980 and from the Diabetes Research Foundation, Finland.

Conflict of Interest. The authors declare that they have no conflict of interest.

References

1. Mukai E, Toyoda K, Kimura H et al (2009) GLP-1 receptor antagonist as a potential probe for pancreatic beta-cell imaging. Biochem Biophys Res Commun 389:523–526
2. Wu Z, Kandeel F (2010) Radionuclide probes for molecular imaging of pancreatic beta-cells. Adv Drug Deliv Rev 62:1125–1138
3. Holst JJ, Deacon CF, Vilsbøll T et al (2008) Glucagon like peptide-1, glucose homeostasis and diabetes. Trends Mol Med 14:161–168
4. Nielsen LL, Young AA, Parkes DG (2004) Pharmacology of exenatide (synthetic exendin-4): a potential therapeutic for improved glycemic control of type 2 diabetes. Regul Pept 117:77–88
5. Tornehave D, Kristensen P, Rømer J et al (2008) Expression of the GLP-1 receptor in mouse, rat, and human pancreas. J Histochem Cytochem 56:841–851
6. Xu G, Doris A, Stoffers DA, Habener JF, Bonner-Weir S (1999) Exendin-4 stimulates both β-cell replication and neogenesis, resulting in increased β-cell mass and improved glucose tolerance in diabetic rats. Diabetes 48:2270–2276
7. Reubi JC, Waser B (2003) Concominant expression of several peptide receptors in neuroendocrine tumours: molecular basis for in vivo multireceptor tumour targeting. Eur J Nucl Med Mol Imaging 30:781–793
8. Körner M, Stöckli M, Waser B, Reubi JC (2007) GLP-1 receptor expression in human tumors and human normal tissues: potential for in vivo targeting. J Nucl Med 48:736–743
9. Wild D, Christ E, Caplin ME et al (2011) Glucagon-like peptide-1 versus somatostatin receptor targeting reveals 2 distinct forms of malignant insulinomas. J Nucl Med 52:1073–1078
10. Gotthardt M, Lalyko G, van Eerd-Vismale J et al (2006) A new technique for in vivo imaging of specific GLP-1 binding sites: first results in small rodents. Regul Pept 137:162–167

11. Wild D, Béhé M, Wicki A et al (2006) [Lys^{40}(Ahx-DTPA-^{111}In)NH$_2$]Exendin-4, a very promising ligand for glucagon-like peptide-1 (GLP-1) receptor targeting. J Nucl Med 47:2025–2033
12. Brom M, Oyen WJ, Joosten L et al (2010) ^{68}Ga-labeled exendin-3, a new agent for the detection of insulinomas with PET. Eur J Nucl Med Mol Imaging 37:1345–1355
13. Wu Z, Todorov I, Li L et al (2011) In vivo imaging of transplanted islets with ^{64}Cu-DO3A-VS-Cys^{40}-exendin-4 by targeting GLP-1 receptor. Bioconjug Chem 22:1587–1594
14. Connolly BM, Vanko A, McQuade P et al (2011) Ex vivo imaging of pancreatic beta cells using a radiolabeled GLP-1 receptor agonist. Mol Imaging Biol 14:79–87
15. Gao H, Niu G, Yang M et al (2011) PET of insulinoma using ^{18}F-FBEM-EM3106B, a new GLP-1 analogue. Mol Pharm 8:1775–1782
16. Kiesewetter DO, Gao H, Ma Y et al (2012) ^{18}F-radiolabeled analogs of exendin-4 for PET imaging of GLP-1 in insulinoma. Eur J Nucl Med Mol Imaging 39:463–473
17. Fani M, Del Pozzo L, Abiraj K et al (2011) PET of somatostatin receptor-positive tumors using ^{64}Cu- and ^{68}Ga-somatostatin antagonists: the chelate makes the difference. J Nucl Med 52:1110–1118
18. McCarthy DW, Shefer RE, Klinkowstein RE et al (1997) Efficient production of high specific activity ^{64}Cu using a biomedical cyclotron. Nucl Med Biol 24:35–43
19. Avila-Rodriguez MA, Nye JA, Nickles RJ (2007) Simultaneous production of high specific activity ^{64}Cu and ^{61}Co with 11.4 MeV protons on enriched ^{64}Ni nuclei. Appl Radiat Isot 65:1115–1120
20. Rajander J, Schlesinger J, Avila-Rodriguez MA, Solin O (2009) Increasing specific activity in Cu-64 production by reprocessing the Ni-64 target material. J Labelled Comp Radiopharm 52:234
21. Någren K, Halldin C (1998) Methylation of amide and thiol functions with [^{11}C]methyl triflate, as exemplified by [^{11}C]NMSP, [^{11}C]Flumazenil and [^{11}C]Methionine. J Labelled Comp Radiopharm 41:831–841
22. Howell RW, Wessels BW, Lovinger R (1999) The MIRD perspective 1999. J Nucl Med 40:3–10
23. Stabin MG, Sparks R, Crowe E (2005) OLINDA/EXM: the second generation personal computer software for internal dose assessment in nuclear medicine. J Nucl Med 46:1023–1027
24. Wild D, Mäcke H, Christ E et al (2008) Glucagon-like peptide 1-receptor scans to localize occult insulinomas. N Engl J Med 359:766–768
25. Christ E, Wild D, Forrer F et al (2009) Glucagon-like peptide-1 receptor imaging for localization of insulinomas. J Clin Endocrinol Metab 94:4398–4405
26. Pattou F, Kerr-Conte J, Wild D (2010) GLP-1-receptor scanning for imaging of human beta cells transplanted in muscle. N Engl J Med 363:1289–1290
27. Andralojc K, Srinivas M, Brom M et al (2012) Obstacles on the way to the clinical visualisation of beta cells: looking for the Aeneas of molecular imaging to navigate between Scylla and Charybdis. Diabetologia 55:1247–1257
28. Blomberg BA, Moghbel MC, Alavi A (2012) PET imaging of β-cell mass: is it feasible? Diabetes Metab Res Rev 28:601–602
29. Sweet IR, Cook DL, Lernmark A et al (2004) Non-invasive imaging of beta cell mass: a quantitative analysis. Diabetes Technol Ther 6:652–659
30. Selvaraju RK, Velikyan I, Johansson L et al (2013) In vivo imaging of the glucagon like peptide 1 receptor in the pancreas with ^{68}Ga-labeled DO3A-exendin-4. J Nucl Med 54:1–6
31. Schmidtler J, Dehne K, Allescher HD et al (1994) Rat parietal cell receptors for GLP-1-(7-36) amide: Northern blot, cross-linking, and radioligand binding. Am J Physiol 267:G423–432
32. Schmidtler J, Schepp W, Janczewska I et al (1991) GLP-1-(7-36) amide, -(1-37), and (1-36) amide: potent cAMP-dependent stimuli of rat parietal cell function. Am J Physiol 260:G940–950
33. Holst JJ (2000) Gut hormones as pharmaceuticals from enteroglucagon to GLP-1 and GLP-2. Regul Pept 93:45–51
34. Vegt E, Melis M, Eek A et al (2011) Renal uptake of different radiolabelled peptides is mediated by megalin: SPECT and biodistribution studies in megalin-deficient mice. Eur J Nucl Med Mol Imaging 38:623–632
35. Wessels BW, Konijnenberg MW, Dale RG et al (2008) MIRD pamphlet No. 20: the effect of model assumptions on kidney dosimetry and response—implications for radionuclide therapy. J Nucl Med 49:1884–1899